

# Linearity Improvement of GaN HEMT for Wireless Communication Applications

Kazutaka INOUE\*, Hiroshi YAMAMOTO, Ken NAKATA, Fumio YAMADA, Takashi YAMAMOTO and Seigo SANO

For GaN HEMTs to be widely used for microwave amplifiers such as point-to-point backhaul systems, good linearity is required. This paper describes our recent achievement in improving linearity by using a newly constructed large signal model of a 0.4  $\mu\text{m}$  GaN HEMT. The model analysis revealed that the intermodulation distortion (IMD) at a backed-off region of more than 10 dB is determined by the sub-threshold  $g_m$  profile; in other words, steep rising  $g_m$  profile degrades IMD. We created a GaN HEMT that has a thin  $n$  layer inserted in the buffer (ini-buffer) structure, and achieved a significant IMD improvement in the backed-off region of more than 8 dB.

Keywords: GaN HEMT, linearity,  $g_m$ , large signal model, microwave

## 1. Introduction

Gallium Nitride (GaN) is desirable material for the application of high-power and high-speed operation electron devices because of its excellent properties such as large energy band gap and high saturated electron velocity. We have released the GaN high electron mobility transistors (HEMTs) on SiC substrate, mainly targeting for the amplifiers of the base station transmitter systems (BTSs) at the frequency range of below 3 GHz. GaN HEMTs have become widely employed to the modern BTS amplifiers such as long-term evolution (LTE), which requires the high output power with excellent efficiency.

Figure 1 shows a schematic illustration of the present communication infrastructure network. Among them, point-to-point (P-to-P) backhaul network systems require the high-power and high-efficiency devices, although GaAs devices have been used in these communication systems. GaN HEMT is suitable for such high-frequency and high-power applications including P-to-P systems, thus many efforts have been dedicated to the development.

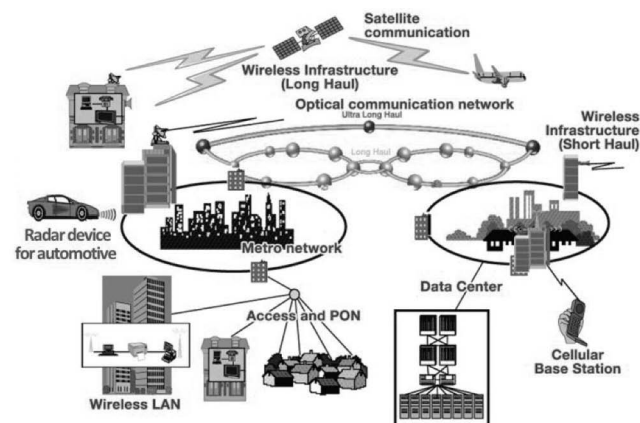


Fig. 1. Present communication infrastructure network

The modern digital telecom systems require the excellent linearity to the amplification devices, to realize the high bit-rate data transformation. In the case of the BTS systems, the distortion cancelling techniques, such as the digital-pre-distortion (DPD), have been widely adopted to suppress the non-linearity of the amplification device. The situation of the P-to-P backhaul amplifier is quite different. The higher frequency amplification makes it difficult to adopt the linearization techniques. In addition, the system does not allow increasing complexity of the amplifier systems. Therefore, pre-distortion techniques are not effective or applicable for P-to-P systems, or in other words, the amplifier device for P-to-P is required high linearity in itself. This paper describes our study for the linearity improvement of the GaN HEMT.

## 2. Linearity of GaN HEMT

The intermodulation distortion (IMD) is one of the useful indexes to estimate the linearity. In the IMD evaluation, 2 tone input signals of the frequency of  $f_1$  and  $f_2$  are used and the input vs. output property is measured. In the ideal case, the frequency components of only  $f_1$  and  $f_2$  are observed (Fig. 2 (a)). While in the actual amplification, the frequency components besides  $f_1$  or  $f_2$  are found in the output signals (Fig. 2 (b)), which are the IMD signal components. For example, the 3rd order components of IMD signals (IM3) emerge at the frequencies of  $2f_1-f_2$  and  $2f_2-f_1$

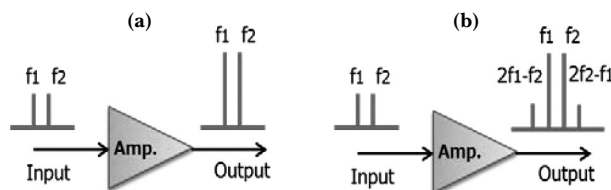
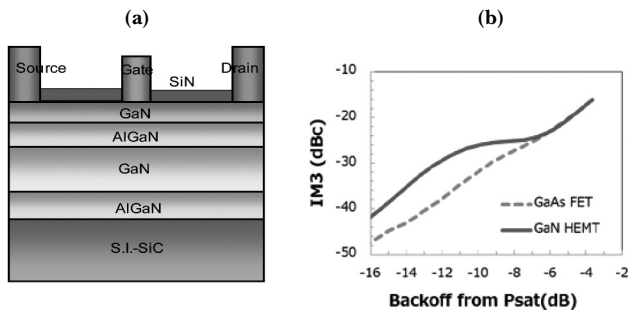


Fig. 2. (a) Ideal amplifier (b) Actual amplifier

as shown in **Fig. 2 (b)**, and these power levels correspond to the degree of the non-linearity.

This study has been done, based on the GaN HEMT structure as shown in **Fig. 3 (a)**. Actually, the AlGaIn/GaN epitaxial structure was grown on the 4 inch semi-insulating SiC substrate by utilizing Metal Organic Chemical Vapor Deposition (MOCVD). The gate length was set to 0.4  $\mu\text{m}$  and the AlGaIn barrier layer thickness was tuned by referring the maximum drain current ( $I_{\text{max}}$ ) versus the pinch off property of the channel.



**Fig. 3.** (a) Conventional GaN HEMT (b) IMD property

GaN exhibits two times higher saturated electron velocity and eight times larger critical breakdown field than those of GaAs. IM3 of below -40 dBc is supposed to be required to the P-to-P systems, and the class-A operation is ideal to realize such excellent IM3 performance. As already mentioned, GaN HEMT realizes higher output power density by utilizing the higher voltage operation. Actually, the typical operation voltage of GaN HEMT is 24 V, and realizes about ten times larger power density than that of GaAs FET. The higher voltage operation also forces GaN HEMT deep class-AB operation to keep equivalent DC power consumption to 10 V biased and class-A operation GaAs FET.

**Figure 3 (b)** shows the typical IM3 profiles of the GaN HEMT of 24 V and class-AB operation, and GaAs FET of 10 V and class-A operation. The IM3 profile of the GaN HEMT exhibits the plateau profile, while the GaAs FET shows the plateau-less profile. The plateau-less profile of class-AB GaN HEMT is essential to replace the GaAs FET in the P-to-P application. Thus, we set the goal to realize the plateau-less profile and started with the GaN HEMT model construction and the operation analysis.

### 3. Model Construction and Analysis

Many models have been proposed and utilized for the large signal analysis of microwave transistors. Among them, we focused on Angelov model<sup>(4), (5)</sup> and have constructed the model for our 0.4  $\mu\text{m}$  GaN HEMT. Angelov model features the straightforward expression utilizing the equivalent circuit parameters, and relatively short computing time to complete the analysis.

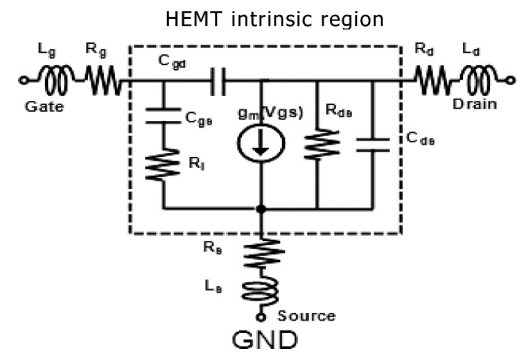


**Fig. 4.** Small-signal equivalent circuit model

The outline of the model construction is as follows. Firstly, the multi-bias S-parameters were measured at various bias conditions, and then small-signal equivalent circuit parameters were extracted. **Figure 4** shows the small-signal equivalent circuit for the analysis. **Figure 5** shows the extracted result of  $g_m$  as a function of the extrinsic gate voltage ( $V_g$ ) and the extrinsic drain voltage ( $V_d$ ). The unit gate width ( $W_{\text{gu}}$ ) of the measured pattern was 50  $\mu\text{m}$  and the total gate width ( $W_{\text{gt}}$ ) was 300  $\mu\text{m}$ . For a large-signal modeling,  $g_m$ ,  $C_{\text{gs}}$ ,  $C_{\text{gd}}$ , and  $R_{\text{ds}}$  were treated as non-linear parameters, while the others were as the linear ones.

The DC modeling was also performed by treating  $g_m$  and  $R_{\text{ds}}$  as non-linear elements. In modeling a GaN HEMT, taking into consideration of the current collapse is one of

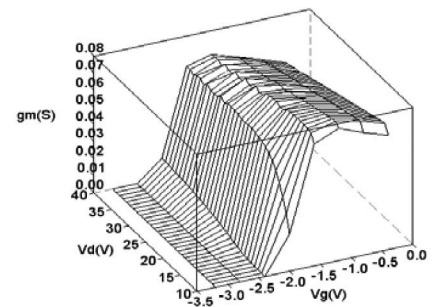


**Fig. 5.** Extracted  $g_m$  vs. extrinsic  $V_g$ ,  $V_d$

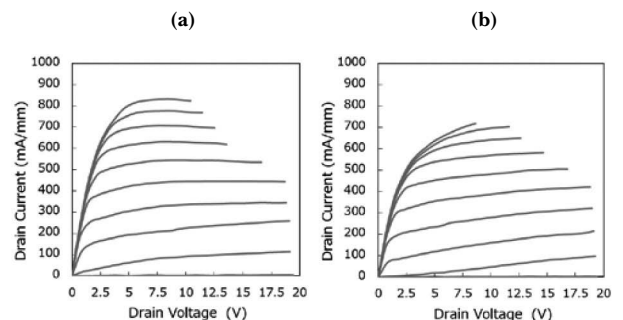


**Fig. 6.** (a) IV without voltage stress (b) IV with voltage stress

the key issues to establish its accuracy. The measurements were done by the  $\mu$ -second order of pulsed signals, and the quiescent drain bias was set to 24 V, which is the typical drain voltage in our targeted operation. The drain current was modeled as the following Angelov formula:

$$I_{ds} = IPK0 \times (1 + \tanh(\Psi)) \times \tanh(\alpha \times V_{ds}) \times (1 + LAMBDA \times V_{ds} + LSB0 \times \exp(V_{dg} - VTR)) \quad (1)$$

where IPK0,  $\Psi$ ,  $\alpha$ , LAMBDA, LSB0, and VTR are the fitting parameters as defined in (5).

The harmonic-balance analysis at the drain bias of 24 V, the drain current of 10% of  $I_{max}$  and the frequency of 10 GHz has been done using the obtained parameters. **Figure 7 (a)** shows the simulated 2-tone Pin-Pout property, and **Fig. 7 (b)** shows the IM3 profiles. The obtained results are in accordance with the measured profiles up to the input power level of 10 dBm. Through this comparison, we concluded the constructed model is appropriate for the intended linearity analysis.

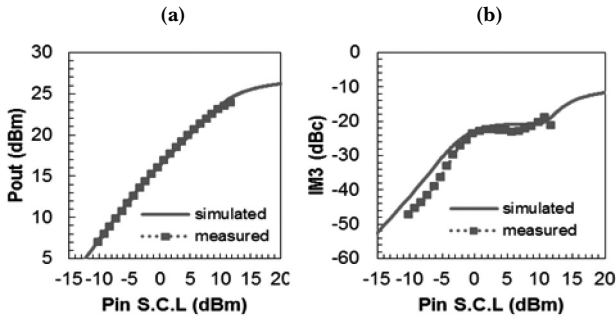


Fig. 7. (a) Pin-Pout profile (b) IM3 profile

Then, the analysis to improve the linearity of the GaN HEMT of class-AB operation was performed. It is commonly recognized that the non-linearity originates in the amplitude or the phase, and the amplitude non-linearity is strongly affected by the  $g_m$  profile. Thus, our analysis is focused on the  $g_m$  property at first. **Figure 8** shows the time domain  $g_m$  profiles at the several characteristic RF input levels.

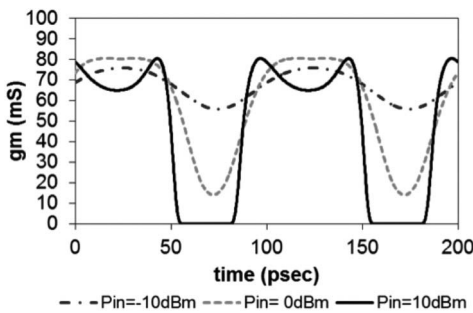


Fig. 8. Time domain  $g_m$  profile

The time-domain  $g_m$  plot of rather small signal case ( $P_{in} = -10$  dBm) exhibits approximately sinusoidal shape. In the case of the input power level of 0 dBm, the maximum region is clipped at first. And then, the plot of the input power of +10 dBm that shows the minimum side of the  $g_m$  profile is also clipped. The maximum, average and minimum values of the analyzed  $g_m$  profiles were plotted in **Fig. 9**. Through the careful comparison of **Fig. 8** and **Fig. 9**, the on-state clipping power level is around -5 dBm, and the off-state clipping is around +2 dBm.

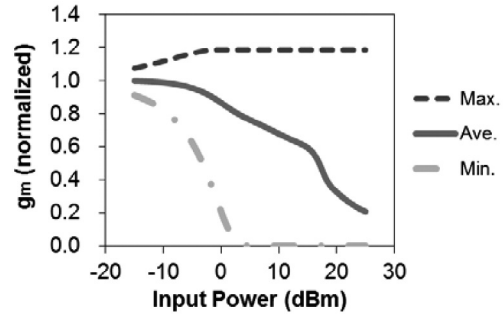


Fig. 9. Analyzed  $g_m$  plot versus input power

**Figure 10** shows the obtained  $g_m$  profile through the measurements and the analysis. The solid circle ( $\bullet$ ) shows the quiescent bias point and the RF swing occurs in accordance with the input power levels.

At first, we assumed the complex on-state  $g_m$  warping corresponds to the inferior IM3 property of the GaN HEMT. Therefore, we set the rectangle  $g_m$  profile as shown in **Fig. 10** and analyzed the IM3 profile. On the contrary to the assumption, the analyzed IM3 profile of the rectangle  $g_m$  case rather degraded around the 15 dB backed off region as shown in **Fig. 11**. The rectangle  $g_m$  enhances the plateau shape of the IM3 profile. In addition, it is revealed through the analysis that the marked region in **Fig. 11** corresponds to the abrupt  $g_m$  rising region from off- to on-state in **Fig. 10**.

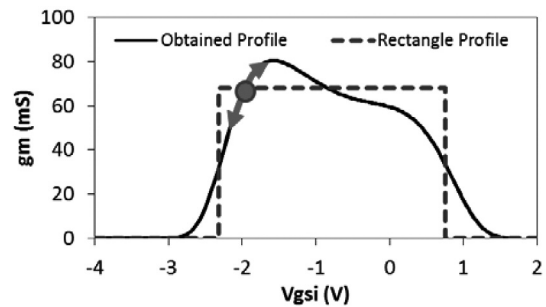


Fig. 10.  $g_m$  profiles

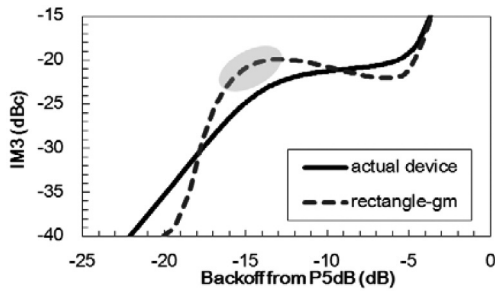


Fig. 11. IM3 analysis of rectangle  $g_m$  case

These analytical results suggest the gradual  $g_m$  rising profile is desirable for the better backed off IM3 profile, in other words, the plateau less profile.

#### 4. GaN HEMT Fabrication and Measurement

The  $g_m$  rising of the GaN HEMT is intrinsically abrupt, by reflecting the extremely high electron density generated from the strong polarization effects. The thin n-GaN layer inserted structure as shown in Fig. 12 is proposed and fabricated to realize the gradual  $g_m$  rising profile. An AlGaIn layer and an intentionally undoped GaN buffer layer were grown, and subsequently an AlGaIn barrier layer and a GaN cap layer were grown, in the case of our conventional structure. In this study, a thin heavily Si-doped GaN layer was inserted in the GaN buffer layer (Fig. 12).

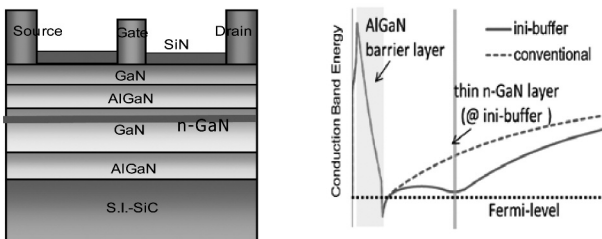


Fig. 12. Developed GaN HEMT structure and band diagram

The inserted thin n-GaN layer modulates the band diagram and the 2DEG distribution in the channel. Figure 13 shows the  $g_m$  profile of our conventional and the ini-buffer structure. The slope of the sub-threshold region is drastically changed by inserting a thin n-GaN layer. The extracted 3<sup>rd</sup> order term of the drain current power series ( $g_{m3}$ ) are plotted in Fig. 14.

The corresponding IM3 results are shown in Fig. 15. The reduction of the non-linearity in the sub-threshold  $g_m$  improves the IM3 of 12 dB-backed off region by 8 dB.

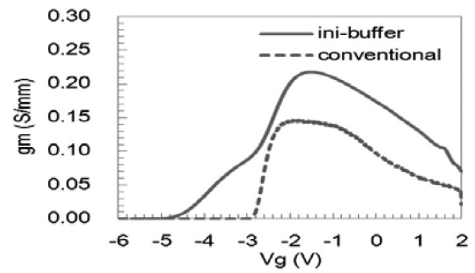


Fig. 13.  $g_m$  profile of ini-buffer structure

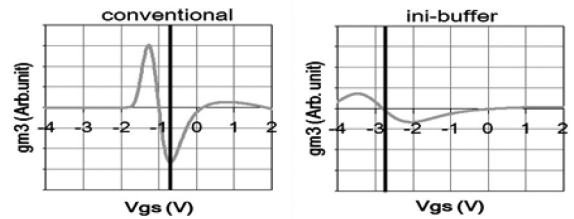


Fig. 14. 3rd order term profile of  $g_m$  power series

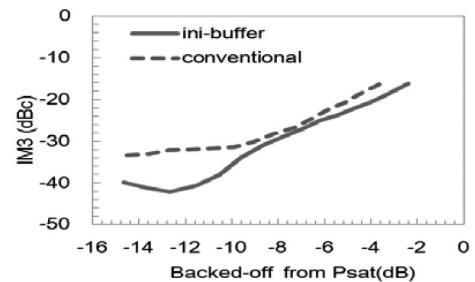


Fig. 15. IM3 profile of ini-buffer structure

#### 5. Conclusion

The linearity improvement has been studied to adopt GaN HEMTs to point-to-point backhaul amplifier applications. A large-signal model of our 0.4  $\mu\text{m}$  AlGaIn/GaN HEMT was developed by considering the 24 V pulse biased operation. This model analysis clarifies the IM3 property of class-AB operation of more than 10 dB backed off region is strongly affected by the sub-threshold  $g_m$  profile. Thus, we fabricated a thin n-GaN inserted buffer structure (ini-buffer structure) standing on the above analysis, which exhibited the significant IM3 improvement by 8 dB at the 12 dB backed off point.

We continue to develop even higher-power and higher-frequency GaN HEMT devices.

### Technical Terms

- \*1 HEMT (High Electron Mobility Transistor): One of the field effect transistors, incorporating a junction between two materials with different band gaps as the channel instead of a doped region. The channel has few collisions with impurities, and is formed with high electron density.
- \*2 S-parameters (Scattering parameters): One of the circuit network parameters which describe the electrical behavior of the high frequency circuits and parts.

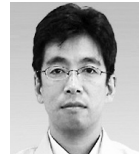
### References

- (1) T. Kikkawa, T. Maniwa, H. Hayashi, M. Kanamura, S. Yokokawa, M. Nishi, N. Adachi, M. Yokoyama, Y. Tateno, and K. Joshin, "An over 200-W output power GaN HEMT push pull amplifier with high reliability," *2004 IEEE MTT-S IMS Digest*, pp. 1347-1350 (2004)
- (2) H. Deguchi, N. Watanabe, A. Kawano, N. Yoshimura, N. Ui, K. Ebihara, "A 2.6GHz Band 537W Peak Power GaN HEMT Asymmetric Doherty Amplifier with 48% Drain Efficiency at 7dB," *2012 IEEE-MTTs-IMS Digest*, pp. 139 (2012)
- (3) N. Ui, H. Sano and S. Sano, "A 80W 2-stage GaN HEMT Doherty Amplifier with -50dBc ACLR, 42% Efficiency 32dB Gain with DPD for W-CDMA Base Station," *2007 IEEE MTT-S IMS Digest*, pp. 1259-1262 (2007)
- (4) I. Angelov, H. Zirath, and N. Rorsman, "A new empirical nonlinear model for HEMT and MESFET devices," *IEEE Tran. Microwave Theory Tech.*, vol. 40, pp. 2258-2266 (December 1992)
- (5) I. Angelov, L. Bengtsson, and M. Garcia, "Extension of the Chalmers nonlinear HEMT and MESFET model," *IEEE Tran. Microwave Theory Tech.*, vol. 44, pp. 1664-1674 (October 1996)
- (6) D. E. Root, "Nonlinear charge modeling for FET large-signal simulation and its importance for IP3 and ACPR in communication circuits," *Proc. 44th IEEE Midwest Circuits Syst. Symp.*, vol. 2, pp. 768-772 (August 2001)
- (7) R. A. Minasian, "Intermodulation Distortion Analysis of MESFET Amplifiers Using the Volterra Series Representation," *IEEE Tran. Microwave Theory Tech.*, vol. 28, pp. 1-8 (January 1980)
- (8) W. Nagy, J. Brown, R. Borges, and S. Singhal, "Linearity Characteristics of Microwave Power GaN HEMTs," *IEEE Tran. Microwave Theory Tech.*, vol. 51, pp. 660-664 (February 2003)
- (9) E. R. Srinidhi, A. Jarndal, and G. Kompa, "A New Method for Identification and Minimization of Distortion Sources in GaN HEMT Devices Based on Volterra Series Analysis," *IEEE Electron Device Lett.*, vol. 28, pp. 343-345 (May 2007)

### Contributors (The lead author is indicated by an asterisk (\*).)

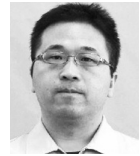
#### K. INOUE\*

- Group Manager, Transmission Devices R&D Laboratories



#### H. YAMAMOTO

- Ph.D.  
Electron Device Development Department, Sumitomo Electric Device Innovations, Inc.



#### K. NAKATA

- Group Manager, Transmission Devices R&D Laboratories



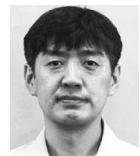
#### F. YAMADA

- Electron Device Development Department, Sumitomo Electric Device Innovations, Inc.



#### T. YAMAMOTO

- Group Manager, Electron Device Development Department, Sumitomo Electric Device Innovations, Inc.



#### S. SANO

- General Manager, Electron Devices Group, Mirco & Opto Devices Division, Sumitomo Electric Asia Ltd.

